analytical chemistry

Article

Cite This: Anal. Chem. 2019, 91, 7411−7417

pubs.acs.org/ac

Direct Measurement of Amorphous Solubility

Jernej Štukelj,*[,†,§] Sami Svanbäck,[†,§] Mikael Agopov,[§] Korbinian Löbmann,[‡] Clare J. Strachan,[†] Thomas Rades,[‡] and Jouko Yliruusi[†,§]

[†]Department of Pharmaceutical Chemistry and Technology, University of Helsinki, Viikinkaari 5E, 00790 Helsinki, Finland

[‡]Department of Pharmacy, University of Copenhagen, Universitetsparken 2, 2100 Copenhagen, Denmark

[§]The Solubility Company Oy, Viikinkaari 6, 00790 Helsinki, Finland

Supporting Information

ABSTRACT: Amorphous materials exhibit distinct physicochemical properties compared to their respective crystalline counterparts. One of these properties, the increased solubility of amorphous materials, is exploited in the pharmaceutical industry as a way of increasing bioavailability of poorly water-soluble drugs. Despite the increasing interest in drug amorphization, the analytical physicochemical toolbox is lacking a reliable method for direct amorphous solubility assessment. Here, we show, for the first time, a direct approach to measure the amorphous solubility of diverse drugs by combining optics with fluidics, the single particle analysis (SPA) method. Moreover, a comparison was made to a theoretical estimation based on thermal analysis and to a standardized supersaturation and precipitation method. We have found a good level of agreement between the three methods. Importantly, the SPA method allowed for the first experimental measurement of the amorphous solubility for griseofulvin, a fast crystallizing drug, without the use of a crystallization inhibitor. In conclusion, the SPA approach enables rapid and straightforward determination of the supersaturation potential for amorphous materials of less than 0.1 mg, which could prove highly beneficial in the fields of materials science, analytical chemistry, physical chemistry, food science, pharmaceutical science, and others.

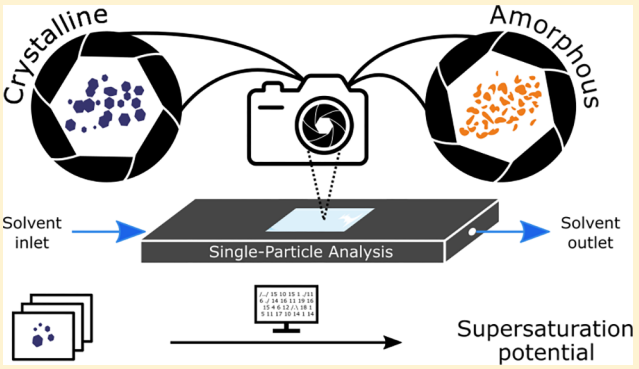

In materials science, amorphous solids lack the three-dimensional long-range order characteristic for crystalline solids. The two materials, having the same molecular composition, possess distinctly different physicochemical properties. The properties of amorphous materials are successfully exploited in many fields, ranging from the electronics, nuclear, chemical, and pharmaceutical industries.[1−6] The pharmaceutical industry is exploiting one specific property of amorphous materials, their increased solubility compared to the respective crystalline materials (often referred to as "apparent solubility"), to enhance the bioavailability of poorly water-soluble drugs.[7,8] However, the available physicochemical analytical toolbox lacks a method that would enable direct measurement of amorphous solubility, the maximum drug concentration in solution upon dissolution of amorphous solid. Here, we use a novel technique, combining the fields of optics and fluidics, to measure amorphous solubility.

Upon dissolution of an amorphous material, a supersaturated solution with a higher chemical potential (μ_{sup}) compared to a solution at thermodynamic equilibrium (μ_{eq}) is generated (eq 1).[9−12] The difference in chemical potential ($\Delta\mu$) is defined as shown in eq 2, where R is the gas constant, T is the temperature, and a_{sup} and a_{eq} are the activity of the solute in a supersaturated state and at the thermodynamic equilibrium, respectively.[13] For sufficiently dilute solutions, the activities of the solute in the supersaturated and equilibrium states can be replaced by the respective concentrations of the solute. Therefore, eq 2 can be written as eq 3, where C_{sup} is the drug concentration in solution at the point of supersaturation, and C_{eq} is the drug concentration in solution at the thermodynamic equilibrium; the ratio between these two concentrations is the degree of supersaturation (DS).

$$\Delta\mu = \mu_{sup} - \mu_{eq} \tag{1}$$

$$\Delta\mu = RT\ln\left(\frac{a_{sup}}{a_{eq}}\right) \tag{2}$$

$$\Delta\mu = RT\ln\left(\frac{C_{sup}}{C_{eq}}\right) = RT\ln(\mathrm{DS}) \tag{3}$$

Received: March 18, 2019
Accepted: May 3, 2019
Published: May 3, 2019

DOI: 10.1021/acs.analchem.9b01378
Anal. Chem. 2019, 91, 7411−7417

Before the maximum DS in solution is reached, crystallization of solute molecules can occur. This phenomenon has resulted in difficulties in experimentally determining the maximum DS of amorphous solids when using classical dissolution experiments, as observed by Murdande et al.[10,14]

The maximum DS can alternatively be estimated from data acquired by thermal analysis of the crystalline and respective amorphous samples. An initial method was developed by Hoffman et al.,[15] and this was later improved by Murdande et al.[10] by taking into account the effects of moisture sorption and ionization. As might be expected, the theoretically estimated amorphous solubilities have been higher than the experimentally achieved values.[9,14,16] Therefore, the accurate experimental measurement of amorphous solubility, especially for fast crystallizing drugs, has gained the general status of "unattainable".[17]

Nevertheless, Almeida et al. reported the first experimental measurement of amorphous solubility of griseofulvin (GRI), a fast crystallizing drug.[18] They assessed amorphous solubility by investigating phase separation phenomena upon precipitation using fluorescent probes. However, a crystallization inhibitor to prevent GRI from crystallizing during the experiment had to be used. Another approach to study drug supersaturation, the standardized supersaturation and precipitation method (SSPM), in which drug predissolved in organic solvent is added to aqueous buffer and the onset of precipitation is detected, was developed by Palmelund et al.[19] The method has been developed for a standardized comparison of supersaturation duration and DS between different compounds under certain conditions, e.g., in biorelevant media or in the presence of precipitation inhibitors, rather than for the exact measurement of the drug's amorphous solubility.

Until now, the direct experimental measurement of amorphous solubility has not been accomplished. The hypothesis that this still is possible is based on the fusion of fluidics and optics, resulting in development of the novel image-based single particle analysis (SPA) method.[20] The method is able to measure the equilibrium solubility of crystalline compounds requiring only a very low amount of material (<0.1 mg) with the measurement starting as soon as the material comes in contact with the solvent.[20,21] During the measurement, particles of interest are entrapped in the flow-through compartment of a specifically designed cell that enables simultaneous extraction of the solvent, maintaining sink conditions, and imaging of the dissolving particles. The obtained images are then further processed with an in-house developed algorithm, and solubility values are generated.

Here, using the SPA method, we show the first direct measurements of amorphous solubility of a diverse range of drugs. Moreover, we compare the results obtained with the SPA method to the theoretically estimated values obtained via thermal analysis, as well as the values estimated with the SSPM method. In this way, we show the suitability of the SPA method for direct measurement of amorphous solubility.

MATERIALS AND METHODS

Materials. Celecoxib (CEL) was acquired from AK Scientific, Inc. (Union City, CA, USA). Danazol (DAN) was acquired from BASF (Ludwigshafen, Germany). Dipyridamole (DIP), GRI, and indomethacin (IND) were acquired from Sigma-Aldrich (St. Louis, MO, USA). These compounds were selected to represent the acidic, basic, and neutral nature of drug compounds. Moreover, the selected compounds can be made amorphous without significant degradation by melting and cooling. GRI was also selected due to its fast crystallization kinetics from the amorphous form.[14,18]

Preparation of Amorphous Forms. The received crystalline forms of the compounds were heated in an aluminum sample holder on a hot plate to slightly above their respective melting points until complete melting was observed. The melt was then immersed in liquid nitrogen and placed in a desiccator over phosphorus pentoxide. After the nitrogen had evaporated, the sample was equilibrated to room temperature and gently ground with a mortar and pestle before being further analyzed.

Differential Scanning Calorimetry (DSC). DSC experiments were performed using a DSC823e (Mettler-Toledo, Greifensee, Switzerland) equipped with a refrigerated cooling system (Julabo FT 900, Seelbach, Germany). Nitrogen was used as a purge gas (50 mL/min).

Samples of 5−10 mg were tightly packed into standard aluminum crucibles (40 μL) with pierced lids. The samples were equilibrated at 25 °C for 3 min and then linearly heated with a heating rate of 10 °C/min to 20 °C above their respective melting points. Measurements of both amorphous and crystalline samples were recorded in triplicate, and thermal events were analyzed using the STARe software (Mettler-Toledo, Greifensee, Switzerland). Temperatures and melting enthalpies were used to estimate the free energy difference between the amorphous and crystalline forms.

X-ray Powder Diffraction (XRPD). XRPD diffractograms were recorded using an Aerius diffractometer (Malvern Panalytical B.V., Almelo, The Netherlands) using Cu Kα radiation (λ = 1.540598 Å) and a divergence slit of 0.5°. Samples were packed into aluminum sample holders and measured with a step size of 0.0066° at 40 kV and 7.5 mA from 5° to 35° (2θ). Measurements were performed in triplicates with independent samples.

Dynamic Water Sorption (DVS). The water sorption isotherms of the five amorphous drug samples were determined using the method previously described by Murdande et al.[10] A VTI-SA+ Vapor Sorption Analyzer (TA Instruments, New Castle, DE, USA) was used to measure the moisture sorption profiles of the amorphous samples. Approximately 10 mg of amorphous sample was placed into a glass holder. To reduce the possibility of sample crystallization during the measurement, no drying step was used. The DVS measurements were performed at 25 °C from 0 to 95% relative humidity (in 10% steps up to 90%). The equilibrium criterion was 0.001% weight change in 5 min with a maximum step time of 150 min. The instrument is calibrated once a month.

Dissolution Media. HCl and borate buffers (pH 2.0 and pH 9.0, respectively) were prepared according to the United States Pharmacopeia (Solutions/Buffer Solutions). Milli-Q water was obtained with the Milli-Q Integral 15 system (MilliporeSigma, Burlington, MA, USA).

Equilibrium Solubility. The equilibirum solubilities of the five model compounds were measured employing a shake-flask method, using a μDISS Profiler (Pion Inc., Billerica, MA, USA) at 22 °C. For CEL, DAN, GRI, and IND, an excess amount of crystalline compound was added to 10 mL of USP pH 2.0 buffer. For DIP, an excess amount of crystalline compound was added to 10 mL of USP pH 9.0 buffer. The excess amount for all compounds was 2.2 ± 0.2 mg and the buffer's pH was selected such that the intrinsic solubility, i.e., the solubility of

DOI: 10.1021/acs.analchem.9b01378
Anal. Chem. 2019, 91, 7411−7417

the un-ionized form, was measured. The concentrations of all compounds were measured, at least in triplicate, until a plateau in the dissolution curve was reached. Each probe of the μDISS device was individually calibrated for each compound. The area under the curve of the second derivative of absorbance was used for calibration in order to avoid interference of the excess drug. Experimental settings are listed in Table S1.

Supersaturation Study Using SSPM. Determination of the initial dimethyl sulfoxide (DMSO) concentration (C100%) for the supersaturation studies was done as described by Palmelund et al.[19] First, the C100% stock solution of each compound was determined such that addition of 200 μL of the compound in the DMSO solution to the buffer would result in precipitation within 1−5 min. Consecutively, stock solutions that resulted in C87.5%, C75.0%, and C50.0% upon addition of 200 μL of predissolved drug in DMSO to 10 mL of the buffer were prepared. Additionally, stock solutions corresponding to C30.0% for CEL and, C60.0% for DIP and GRI were prepared. The total volume of DMSO added was kept at 2% for all experiments. Upon spiking the buffer with the stock solution, the concentration was monitored in situ with the μDISS Profiler (Pion Inc., Billerica, MA, USA) by using the area under the curve of the second derivative of the UV absorbance for 60 min or longer, if no precipitation had occurred.

The determination of induction time of precipitation (t_{ind}) is limited by the experimental conditions.[19] Here, a slightly different approach to that originally proposed by Palmelund et al. to determine t_{ind} was developed.[19] The time-point of the sharpest decrease in concentration was determined as the local minimum of the first derivative of the concentration versus time plot using Matlab software (MathWorks, Natick, MA, US) (Figure S1). The crystallization rate was subsequently calculated using the slope of the linear trend-line fitted to 12 data points around the point of the steepest decrease in concentration. Consequently, the t_{ind} was defined as the point where the fitted trend-line crossed the initial concentration value.

Image-Based SPA Solubility Measurements. Dissolution experiments were conducted using the SPA method as described previously by Svanbäck et al. and Štukelj et al.[21,22] Briefly, the method consists of an image-analysis algorithm and a flow-through setup, which enables imaging of the fixed drug particles under constant flow conditions (Figure S2). The constant flow continuously displaces drug molecules from the surface of the dissolving particle. This enables, via the analysis of the image series, for the concentration of the solute to be measured at the particle-solution interface (for a more detailed description, see Supporting Information S-2). According to the Noyes and Whitney diffusion layer theory, the measured concentration is the thermodynamic equilibrium solubility of a crystalline compound.[22−24] Consequently, with the amorphous material, the concentration at the interface is equal to the maximum achievable drug concentration in solution−amorphous solubility. (Figure 1).

The solubilities of all five crystalline and amorphous samples were measured in triplicate in Milli-Q water. Moreover, the solubilities of CEL, DAN, GRI, and IND were measured in USP buffer pH 2.0, and the solubility of DIP was measured in USP buffer pH 9.0. The obtained solubility values, therefore, were the average of three independent measurements, where at least ten particles per single measurement were analyzed. Additionally, amorphous IND was also measured in HCl buffer pH 2.0 in the presence of 0.1% (w/v) polyvinylpyrolidone (PVP). The additional measurement using PVP was performed in order to assess the need for a crystallization inhibitor in the SPA experiments.

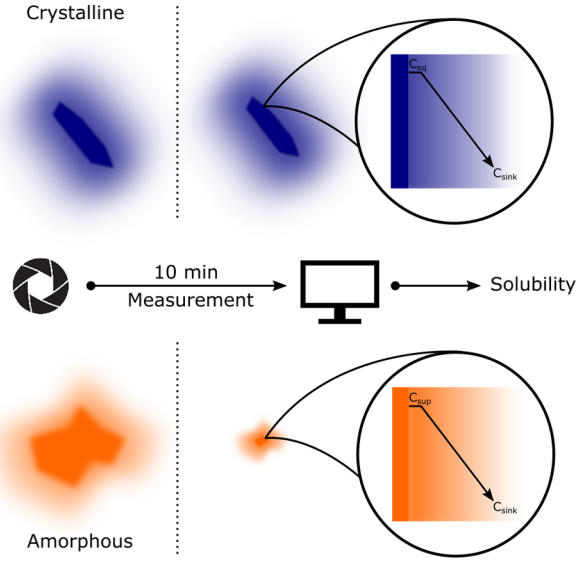

Figure 1. Crystalline and amorphous particle depicted at the beginning and after 10 min of the SPA measurement. As the dissolution occurs in the controlled environment with sink conditions, the only rate limiting step is the concentration at the particle−solution interface. With the thermodynamically most stable crystalline form, the concentration at the interface is equal to the thermodynamic equilibrium concentration. Consequently, with the amorphous material, the concentration at the interface is equal to the maximum achievable drug supersaturation in solution upon amorphization.

RESULTS AND DISCUSSION

Characterization of Solid-State Forms. The results of the solid-state characterization of the five model compounds, in both crystalline and amorphous form, are presented in Figure 2 and summarized in Table 1. The results are in good agreement with previously reported XRPD and DSC data on these compounds.[14,16,25] Furthermore, the XRPD diffractograms of the crystalline forms of DAN, DIP, GRI, and IND match the predicted diffractograms for the corresponding structures in the Cambridge Structural Database (CSD), YAPZEU, BIRKES10, GRISFL, and INDMET01, respectively. For crystalline CEL, the CSD-predicted XRPD powder pattern (DIBBUL) exhibits substantially different relative peak intensities compared to our experimental data, presumably due to preferred orientation effects of the needle shaped particles.[26] Nonetheless, the diffraction pattern of CEL in this study has three sharp diffraction peaks that indicate the thermodynamically stable crystalline form of CEL.[27,28] Amorphous samples were devoid of diffraction peaks, and all showed a glass transition, followed by crystallization and melting (Figure 2 and Table 1).

Validation of the SPA Method. The equilibrium solubilities of the crystalline compounds were measured with the shake-flask method and compared to the equilibrium solubilities measured with the SPA method (Figure 3a). There was no significant difference in the standard deviation for the SPA (M = 0.51 μg/mL, SD = 0.35 μg/mL) and the shake-flask method (M = 0.27 μg/mL, SD = 0.12 μg/mL) conditions; $t(4)$ = 1.72, p = 0.16. A correlation coefficient (R^2) of 0.996 was

DOI: 10.1021/acs.analchem.9b01378
Anal. Chem. 2019, 91, 7411−7417

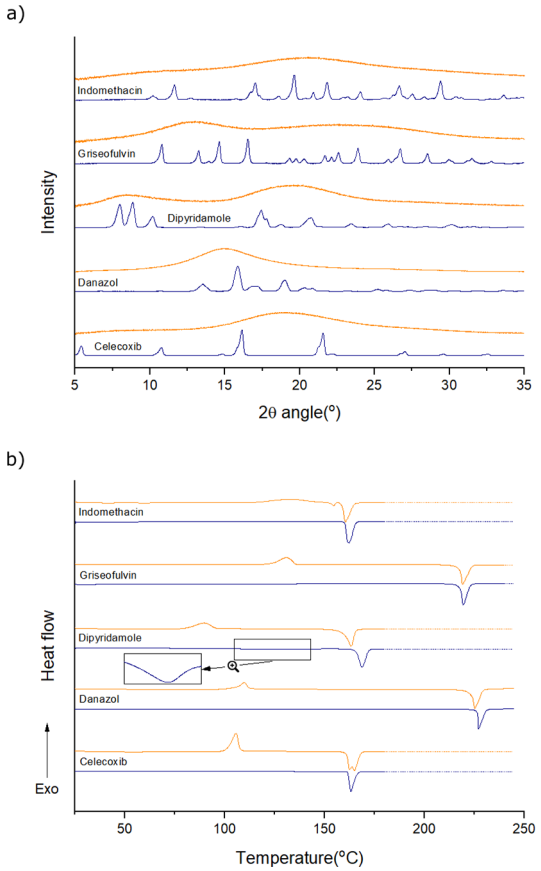

Figure 2. (a) XRPD diffractograms of amorphous (orange) and crystalline (blue) drug samples. (b) DSC thermograms of amorphous (orange) and crystalline (blue) drug samples. The zoomed-in endothermic event for crystalline dipyridamole is due to evaporation of water from the sample.

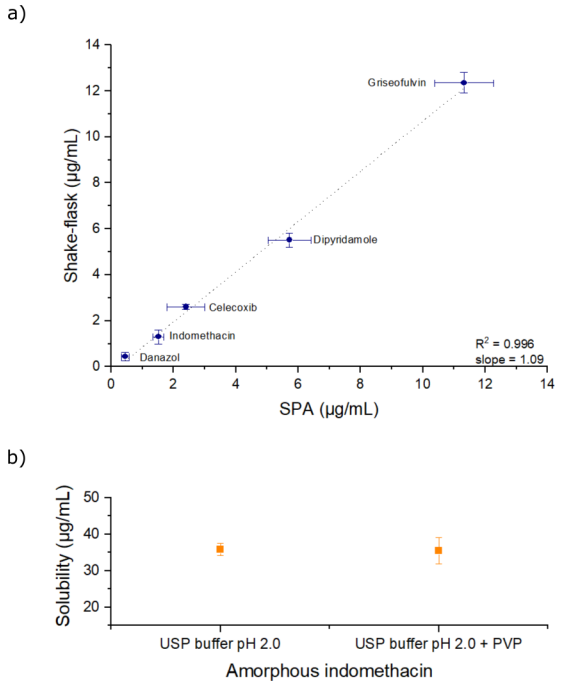

Figure 3. (a) Correlation between the equilibrium solubility measured with the SPA method and the shake-flask method using the μDISS Profiler. (b) Apparent equilibrium solubility of amorphous IND measured in USP buffer pH 2.0 and USP buffer pH 2.0 with added PVP 0.1% (m/v) using the SPA method. Error bars represent one standard deviation.

observed, validating the SPA method for measuring the thermodynamic equilibrium solubility of the selected crystalline model compounds. Moreover, the solubility of amorphous IND was measured in both USP HCl buffer pH 2.0 and the same buffer with PVP (0.1% (w/v)) added (Figure 3b). PVP acts as a crystallization inhibitor during the dissolution of amorphous material.[29] The presence of PVP in the dissolution medium did not affect the solubility of amorphous IND measured with the SPA method. The result suggests that the SPA method is able to directly measure the amorphous solubility of a drug, without the need for crystallization inhibitors.

To rationalize the solubility values for amorphous forms obtained with the SPA method, the amorphous solubilities of the five model drugs were approached in three different ways, (1) theoretical estimation using the Hoffman method corrected for the impact of absorbed water on amorphous solute, (2) indirect measurement using the modified SSPM, and (3) direct measurement with the SPA method. Moreover, a comparison was made also to other attempts of measuring amorphous solubility reported in literature.[10,16,18,31] To facilitate comparison of amorphous solubility between the selected model compounds, the DS with respect to thermodynamic equilibrium solubility was used.

Theoretical Estimation of DS. According to Hoffman, the difference in Gibbs free energy (ΔG) between the crystalline and the amorphous form can be estimated using eq 4.[15] H_m, T_m, and T are the melting enthalpy of the crystalline form, the melting temperature of the crystalline form, and the experimental temperature measured in Kelvin, respectively. Using the ΔG estimation, the maximum DS due to

Table 1. Distinct XRPD Peak Positions, Glass Transition (T_g), and Crystallization Temperatures (T_c) of Amorphous Samples and Temperature of Melting (T_m) and Enthalpy of Melting (ΔH_m) for Crystalline Samples[a]

	XRPD			DSC	
compound	distinct peak positions (°2θ)	T_g (°C)	T_c (°C)	T_m (°C)	ΔH_m (J/g)
celecoxib	5.4, 16.2, 21.6	48.9 ± 1.7	101.2 ± 0.1	161.4 ± 0.2	99.1 ± 1.0
danazol	13.5, 15.8, 18.9	74.2 ± 1.1	105.6 ± 0.2	226.8 ± 0.3	102.5 ± 2.4
dipyridamole	8.1, 8.9, 17.5	41.7 ± 1.3	80.5 ± 2.4	165.6 ± 0.1	60.1 ± 0.9
griseofulvin	10.8, 14.6, 16,5	89.0 ± 1.2	123.3 ± 0.4	217.6 ± 0.3	114.4 ± 2.0
indomethacin	11.6, 17.0, 19.6	36.4 ± 0.6	116.2 ± 0.3	159.8 ± 0.2	102.3 ± 4.5

[a]The T_g value is given as the midpoint temperature of the step change in heat capacity of the DSC thermograms. For T_c and T_m, onset temperatures are listed.

DOI: 10.1021/acs.analchem.9b01378
Anal. Chem. 2019, 91, 7411−7417

Table 2. DS Measured with the SPA Method, the Modified SSPM, and Theoretically Estimated According to the Hoffman Method with Correction for the Effect of Water on the Amorphous Solute, and DS Values Found in the Literature[a]

	SPA method		SSPM	theoretical estimation	literature	
compound	milli-Q[b]	USP buffer	USP buffer	N/A	dissolution in water	theoretical estimation
CEL	18.9	22.3[e]	20.6[e]	21.7	3.1[c,h]	21[g,h]
DAN	18.3	21.9[e]	21.5[e]	23.9	3.0[d,i]	26.5[i]
DIP	15.3	17.2[f]	17.3[f]	6.6		10[k]
GRI	29.8	34.3[e]	5.9[e]	34.6	1.4[d,i]	29.1[i], 30.9[j]
IND	20.4	23.6[e]	22.3[e]	18.7	4.9[d,i]	20.8[i]

[a]CEL, celecoxib; DAN, danazol; DIP, dipyridamole; GRI, griseofulvin; and IND, indomethacin. [b]Milli-Q-ultrapure water, type 1. [c]Distilled water. [d]Deionized water. [e]USP HCl buffer pH 2.0. [f]USP borate buffer pH 9.0. [g]Predicted value below the T_g of the drug. [h]Ref 16. [i]Ref 10. [j]Ref 18. [k]Ref 30.

amorphization was predicted according to Hancock and Parks[9] and corrected for the impact of water on the amorphous solute as proposed by Murdande et al. through eq 5.[10] R and $\exp(-I(a_2))$ are the gas constant and a correction factor obtained from DVS measurements, as shown by Murdande et al.[10] The calculated values are listed in Table 2.

$$\Delta G = \frac{H_m \times (T_m - T) \times T}{T_m^{\,2}} \tag{4}$$

$$\mathrm{DS} = e^{-\Delta G/RT} \times e^{-I(a_2)} \tag{5}$$

Indirect Measurement of DS Using the Modified SSPM. The modified SSPM measurement is considered indirect, since the maximum DS was not directly measured but rather extrapolated. The t_{ind} of each model compound at a certain DS was estimated from the dissolution profile, as described in the Materials and Methods section. DS values for the respective stock solutions of each compound were calculated and plotted against t_{ind} (Figure S3). The fitted curves follow eq 6, derived from classical nucleation theory assuming t_{ind} is inversely proportional to the nucleation rate, with α and β being the two linear coefficients.[19,31,32] In order to estimate the maximum DS, a linear trend line was fitted only to the points that would fall within the horizontal region of the fit according to eq 6 (Figure S4). Otherwise, an estimation of the maximum DS would not be possible, since the nucleation theory results in infinite DS with infinitesimal t_{ind}. The estimated maximum DS values are listed in Table 2.

$$t_{ind} = e^{\alpha+\beta\ln(\mathrm{DS})^{-2}} \tag{6}$$

Direct Measurement of DS Using the SPA Method. The solubilities of the amorphous and crystalline samples were measured in Milli-Q water and USP buffers as soon as the solvent came in contact with particles. The DS upon amorphization was calculated using eq 3. The calculated DS values for each of the model compounds are summarized in Table 2.

Effect of Ionization. The solubility ratio between two polymorphs of the same compound is independent of the solvent used.[33] On the other hand, Murdande et al. proposed an effect of ionization on the DS with respect to amorphous vs crystalline materials.[10] In this study, the USP buffers were used in a way that any possible ionization effect was avoided, and drugs were in their respective un-ionized forms. Furthermore, close agreement between the DS values observed in Milli-Q water and USP buffers with the SPA method was observed (Table 2). No ionization effect on DS was detected with the SPA method; the difference between the DS in Milli-Q and DS in USP buffers is the same for ionizable drugs (CEL, DIP, and IND) as for the neutral drugs (DAN and GRI).

Onset of Crystallization. The literature values for DS upon amorphization obtained with classical dissolution of amorphous material and measurement of concentration overtime are lower than the DS values measured by the SPA method, the modified SSPM, as well as the theoretical estimation (Table 2). The reason for this is that, in classical dissolution measurements, crystallization may start before the maximum DS in solution is reached.[9,10,16] With the modified SSPM, the issue of instantaneous precipitation, when the solution is close to the maximum DS, was avoided by measuring the precipitation onset of solutions with DS below the maximum DS. In contrast to classical dissolution experiments, measurements with the SPA method were conducted as soon as the solvent came in contact with the sample in order to circumvent any possible solid-state transformations during the measurements.

Successful Measurement of DS with the SPA Method. For three compounds, CEL, DAN, and IND, the DS values obtained with the SPA method (22.3, 21.9, and 22.6, respectively), the adapted SSPM method (20.6, 21.5, and 22.3, respectively), and the theoretical estimation (21.7, 23.9, and 18.7, respectively) show high correlation (Table 2). For CEL, the DS range, 7−21, reported in the literature was obtained over a temperature range of 34−75 °C.[18] The relevant temperature range for comparison with this study is below the T_g of the drug, with the predicted DS value of 21 listed in Table 2. In contrast, for DIP, the DS values obtained with the SPA (17.2) and adapted SSPM (17.3) methods are in close agreement, but the theoretically estimated value is significantly lower (6.6).

A possible reason for the inconsistency in DS values for DIP could be the fact that the Hoffman method assumes that the heat capacities (C_p) of the crystalline and amorphous material are the same. The assumption might lead to inaccurate ΔG estimation, especially for compounds with a significant difference in C_p between the crystalline and amorphous forms. An approach that is free of such C_p assumptions was developed by Almeida et al.[18] Nevertheless, despite the assumption of uniform C_p for crystalline and amorphous forms, the Hoffman method has been found to provide a good estimate of the ΔG.[34] Moreover, for another drug used in this study (GRI), the Hoffman method and the approach by Almeida et al. gave similar values of DS upon amorphization (34.6 and 30.9, respectively).

Another reason for the discrepancy between the theoretically estimated and the experimentally measured DS of DIP could be the hygroscopicity of the sample. DIP is highly hygroscopic,

DOI: 10.1021/acs.analchem.9b01378
Anal. Chem. 2019, 91, 7411−7417

which can be observed as evaporation of adsorbed water from the surface of crystalline material leading to the highlighted endothermic event slightly above 100 °C in the DSC plot (Figure 2). Furthermore, the DVS experiment also showed the high affinity of amorphous DIP for water, which resulted in sample mass loss (0.39%) above RH 80%; upon crystallization, water was expelled from the sample resulting in weight loss (Figure S5). The results suggest that the correction for the impact of water on the highly hygroscopic amorphous sample might overcorrect the DS. To follow up on this assumption, the estimated DS based solely on the ΔG, without the correction for the adsorbed water, was calculated. A value of 15.2 was obtained, which is much closer to the experimentally measured DS with the SPA method and the one estimated with the adapted SSPM method.

Amorphous Solubility of the Rapidly Crystallizing GRI. Using the SPA method, without any crystallization inhibitor present in the medium, a DS of 34.3 for GRI was obtained. The DS value was in good agreement with the value estimated according to the Hoffman method (34.6). In contrast, the DS estimated with the modified SSPM was much lower at 5.9. GRI is known for its fast crystallization kinetics, which is most likely the reason for the low maximum DS observed by the adapted SSPM method. This might be prevented with the addition of a crystallization inhibitor, as was done with hydroxypropyl methylcellulose acetate succinate grade HF (HPMCAS-HF) by Almeida et al.[18] They attempted to indirectly measure amorphous solubility by looking at the phase separation phenomena upon precipitation using fluorescent probes as they added drugs dissolved in organic solvent to the aqueous buffers. When using crystallization inhibitors, it is important to evaluate if the obtained higher DS is actually due to inhibition of crystallization and not due to a solubility enhancing effect of these compounds. Nonetheless, the DS for GRI, obtained by Almeida et al. (30.8) is close to that measured with the SPA method (34.3).

CONCLUSION

In this study, we have demonstrated the suitability of the SPA method for direct measurement of solubility of amorphous materials. The amorphous solubilities of five model drug compounds were assessed using three different approaches, the theoretical estimation using the Hoffman method, indirect measurement using the modified SSPM method, and direct measurement using the SPA method. For CEL, DAN, and IND, the amorphous solubility values correlated for all three methods used. For DIP, the theoretically estimated DS was, most likely due to the hygroscopic nature of the sample, and significantly lower when compared to the values obtained with the adapted SSPM and the SPA method, which were in agreement with one another. On the other hand, for GRI, the SPA method was in agreement with the Hoffman method but not the adapted SSPM method due to fast crystallization kinetics of the drug.

The SPA method used in this study represents a new approach for direct experimental measurement of amorphous solubility. The SPA method is especially useful when the material of interest crystallizes quickly upon dissolution, which can mask its true supersaturation potential with established solubility measurement methods. GRI, a fast crystallizing drug, was successfully analyzed in this work, and for the first time, its amorphous solubility was experimentally determined without the use of crystallization inhibitors.

The straightforward approach to measure amorphous solubility using the SPA method provides insights in the supersaturation potential that a certain drug candidate (or indeed any other material) possesses. This, now easily extracted, piece of information is of high value in the drug formulation process and could result in more optimized drug products. Moreover, the method has much potential in the fields of materials science, analytical chemistry, physical chemistry, food science, and other fields where amorphization, solubility, and supersaturation play a significant role.

ASSOCIATED CONTENT

Supporting Information

The Supporting Information is available free of charge on the ACS Publications website at DOI: 10.1021/acs.analchem.9b01378.

Experimental settings of the μDISS device, determination of the induction time in the SSPM experiments, description of the SPA method, DS vs induction time plot, estimation of the maximum DS assessed by the SSPM experiments, and water sorption of amorphous dipyridamole (PDF)

AUTHOR INFORMATION

Corresponding Author

*E-mail: jernej.stukelj@helsinki.fi.

ORCID

Jernej Štukelj: 0000-0002-1452-4310
Korbinian Löbmann: 0000-0002-8710-6347
Clare J. Strachan: 0000-0003-3134-8918
Thomas Rades: 0000-0002-7521-6020

Author Contributions

J.Š., S.S., K.L., C.J.S., T.R., and J.Y. conceived the project and designed the experiments. M.A. helped with the data processing. J.Š. performed the experiments and wrote the manuscript. S.S., K.L., C.J.S., T.R., and J.Y. reviewed the manuscript.

Notes

The authors declare the following competing financial interest(s): J. Štukelj, M. Agopov, S. Svanbäck, and J. Yliruusi are shareholders of The Solubility Company Oy that owns the intellectual property rights to the SPA method.

ACKNOWLEDGMENTS

J.Š. acknowledges funding from the Doctoral Programme in Drug Research (DPDR). The authors acknowledge funding from NordForsk for the Nordic University Hub project #85352 (Nordic POP, Patient Oriented Products). J.Š. acknowledges Jakob Plum for assistance with the μDISS Profiler.

REFERENCES

(1) Wu, C. C.; Liu, T. L.; Hung, W. Y.; Lin, Y. T.; Wong, K. T.; Chen, R. T.; Chen, Y. M.; Chien, Y. Y. *J. Am. Chem. Soc.* **2003**, *125*, 3710−3711.

(2) Osaka, I.; Zhang, R.; Sauvè, G.; Smilgies, D. M.; Kowalewski, T.; McCullough, R. D. *J. Am. Chem. Soc.* **2009**, *131*, 2521−2529.

(3) Noh, M.; Kwon, Y.; Lee, H.; Cho, J.; Kim, Y.; Kim, M. G. *Chem. Mater.* **2005**, *17*, 1926−1929.

(4) Blink, J.; Farmer, J.; Choi, J.; Saw, C. *Metall. Mater. Trans. A* **2009**, *40*, 1344−1354.

DOI: 10.1021/acs.analchem.9b01378
Anal. Chem. 2019, 91, 7411−7417

(5) Benck, J. D.; Chen, Z.; Kuritzky, L. Y.; Forman, A. J.; Jaramillo, T. F. *ACS Catal.* **2012**, *2*, 1916−1923.
(6) Gardner, C. R.; Walsh, C. T.; Almarsson, O. *Nat. Rev. Drug Discovery* **2004**, *3*, 926−934.
(7) Williams, H. D.; Trevaskis, N. L.; Charman, S. A.; Shanker, R. M.; Charman, W. N.; Pouton, C. W.; Porter, C. J. H. *Pharmacol. Rev.* **2013**, *65*, 315−499.
(8) Dengale, S. J.; Grohganz, H.; Rades, T.; Löbmann, K. *Adv. Drug Delivery Rev.* **2016**, *100*, 116−125.
(9) Hancock, B. C.; Parks, M. *Pharm. Res.* **2000**, *17*, 397−404.
(10) Murdande, S. B.; Pikal, M. J.; Shanker, R. M.; Bogner, R. H. *J. Pharm. Sci.* **2010**, *99*, 1254−1264.
(11) Surwase, S. A.; Boetker, J. P.; Saville, D.; Boyd, B. J.; Gordon, K. C.; Peltonen, L.; Strachan, C. J. *Mol. Pharmaceutics* **2013**, *10*, 4472−4480.
(12) Brouwers, J.; Brewster, M. E.; Augustijns, P. *J. Pharm. Sci.* **2009**, *98*, 2549−2572.
(13) Kashchiev, D.; van Rosmalen, G. M. *Cryst. Res. Technol.* **2003**, *38*, 555−574.
(14) Murdande, S. B.; Pikal, M. J.; Shanker, R. M.; Bogner, R. H. *Pharm. Res.* **2010**, *27*, 2704−2714.
(15) Hoffman, J. D. *J. Chem. Phys.* **1958**, *29*, 1192−1193.
(16) Gupta, P.; Chawla, G.; Bansal, A. K. *Mol. Pharmaceutics* **2004**, *1*, 406−413.
(17) Murdande, S. B.; Pikal, M. J.; Shanker, R. M.; Bogner, R. H. *Pharm. Dev. Technol.* **2011**, *16*, 187−200.
(18) Almeida E Sousa, L.; Reutzel-Edens, S. M.; Stephenson, G. A.; Taylor, L. S. *Mol. Pharmaceutics* **2015**, *12*, 484−495.
(19) Palmelund, H.; Madsen, C. M.; Plum, J.; Müllertz, A.; Rades, T. *J. Pharm. Sci.* **2016**, *105*, 3021−3029.
(20) Svänback, S.; Ehlers, H.; Antikainen, O.; Yliruusi, J. *Anal. Chem.* **2015**, *87*, 5041−5045.
(21) Svanbäck, S. Experimental, Results and Discussion. In *Toward accurate high-throughput physicochemical profiling using image-based single-particle analysis*; University of Helsinki: Helsinki, 2016; pp 22−45.
(22) Štukelj, J.; Svanbäck, S.; Strachan, C. J.; Yliruusi, J.; Kristl, J. *Anal. Chem.* **2019**, *91*, 3997−4003.
(23) Dokoumetzidis, A.; Macheras, P. *Int. J. Pharm.* **2006**, *321*, 1−11.
(24) Noyes, A. A.; Whitney, W. R. *J. Am. Chem. Soc.* **1897**, *19*, 930−934.
(25) Baghel, S.; Cathcart, H.; Redington, W.; O'Reilly, N. J. *Eur. J. Pharm. Biopharm.* **2016**, *104*, 59−71.
(26) Vasu Dev, R.; Shashi Rekha, K.; Mohanti, S. B.; Rajender Kumar, P.; Om Reddy, G.; Vyas, K. *Acta Crystallogr., Sect. C: Cryst. Struct. Commun.* **1999**, *55*, IUC9900161. IUC9900161
(27) Ghanavati, R.; Taheri, A.; Homayouni, A. *Mater. Sci. Eng., C* **2017**, *72*, 501−511.
(28) Homayouni, A.; Sadeghi, F.; Varshosaz, J.; Garekani, H. A.; Nokhodchi, A. *Eur. J. Pharm. Biopharm.* **2014**, *88*, 261−274.
(29) Murdande, S. B.; Pikal, M. J.; Shanker, R. M.; Bogner, R. H. *J. Pharm. Sci.* **2011**, *100*, 4349−4356.
(30) Baghel, S.; Cathcart, H.; O'Reilly, N. J. *Int. J. Pharm.* **2018**, *536*, 414−425.
(31) Ozaki, S.; Minamisono, T.; Yamashita, T.; Kato, T.; Kushida, I. *J. Pharm. Sci.* **2012**, *101*, 214−222.
(32) Kuldipkumar, A.; Kwon, G. S.; Zhang, G. G. Z. *Cryst. Growth Des.* **2007**, *7*, 234−242.
(33) Augustijns, P.; Brewster, M. E. Solvent Systems for Crystallization and Polymorph Selection. In *Biotechnology : Pharmaceutical Aspects*; Borchardt, R. T., Middaugh, C. R., Eds.; Springer Science+Business Media: New York, 2007; Vol. *VI*, pp 52−62.
(34) Marsac, P. J.; Konno, H.; Taylor, L. S. *Pharm. Res.* **2006**, *23*, 2306−2316.

DOI: 10.1021/acs.analchem.9b01378
Anal. Chem. 2019, 91, 7411−7417